Available online at www.sciencedirect.com

SciVerse ScienceDirect

Ceramics International 38 (2012) 3553–3562

CERAMICS INTERNATIONAL

www.elsevier.com/locate/ceramint

Effects of $BaTiO_3$ and FeAlSi as fillers on the magnetic, dielectric and microwave absorption characteristics of the epoxy-based composites

Wenhu Yang [a,b], Shuhui Yu [a,*], Rong Sun [a,*], Ruxu Du [a,c]

[a] Shenzhen Institutes of Advanced Technology, Chinese Academy of Sciences, Shenzhen 518055, China
[b] Graduate School of the Chinese Academy of Sciences, Beijing 100039, China
[c] Institute of Precision Engineering, The Chinese University of Hong Kong, Hong Kong, China

Received 30 November 2011; received in revised form 26 December 2011; accepted 27 December 2011
Available online 2 January 2012

Abstract

A systematic study was carried out on the magnetic, dielectric and microwave absorption properties of the two-phase FeAlSi/epoxy and three-phase FeAlSi/$BaTiO_3$/epoxy composites through experimental and simulation method. A percolation effect was observed in the dielectric, but not in the magnetic behavior of the FeAlSi/epoxy composites when the FeAlSi content was high. The 2D modeling shows that the high electric energy density is responsible for the high permittivity near the percolation threshold (49 vol%). On the other hand, the permeability of the composites matches well with the effective medium theory model (EMT), indicating that the permeability of FeAlSi/epoxy composite is more associated with the filler size and shape. Theoretical calculations show that the increment of the FeAlSi and $BaTiO_3$ loading, as well as the thickness will cause the absorption peak position to shift to low frequencies. The microwave absorption of these composites can be mainly attributed to the dielectric loss and magnetic loss.

Keywords: C. Magnetic properties; C. Dielectric properties; FeAlSi; $BaTiO_3$

1. Introduction

A printed circuit board (PCB) is used to mechanically support and electrically connect electronic components using conductive pathways. The number of passive components on the PCB increases dramatically with the increasing complexity of electronic systems. Embedding the passive components into the PCB is an effective way to realize the miniaturization and multifunction of the systems [1,2]. Polymer-dielectric composites have been proposed as the embedded capacitor materials because of their flexibility, good processability and tailorable performance by controlling the content of the filler. Various dielectric particles including high permittivity ceramics ($BaTiO_3$ [3,4], $CaCu_3Ti_4O_{12}$ [5] and PZT [6]) metallic particles (Ni, Fe, Co, Al, Ag) [7,8], as well as the carbon nanotube [9] and graphene [10] have been employed as the dielectric fillers. Studies [11–13] have shown that the dielectric properties of the polymer composites are significantly dependent on the shape, size, and the conductivity of the fillers. The interface properties [14] also strongly affect the dielectric behavior because interfaces act as the charge carrier trapping sites, which determine the charge carrier transport and storage.

Polymer-magnetic composites [15,16] have also been studied to explore the potential applications in embedded inductors. Fe_3O_4 [17] and other ferrites [18] are employed as the magnetic fillers. Similar with the polymer-dielectric composite, the permeability of these composites is dependent on the magnetic property and the loading of fillers. Li et al. [19] has reported a $Ba_3Co_2Fe_{23}O_{41}$/PVDF composite with the initial permeability increasing from about 1 to 2.5 (500 MHz) while the volume fraction of the $Ba_3Co_2Fe_{23}O_{41}$ was increased up to 50 vol%. Shirakata et al. [20] have reported a Zn–Ni–Fe/polymer composite and found that the real permeability is dependent on the magnetic filler loading. However, Thomas et al. [21] have investigated various polymer magnetic composites and found that the more significant method to obtain the high permeability composite was introducing high permeability fillers rather than increasing loading content.

* Corresponding authors.
E-mail addresses: yuushu@gmail.com (S. Yu), rong.sun@siat.ac.cn (R. Sun).

0272-8842/$36.00
doi:10.1016/j.ceramint.2011.12.071

In recent years, the composites containing both dielectric and magnetic particles [22] were proposed to meet the request of the multi-functional materials. Compared with the two phase dielectric-polymer or magnetic-polymer composites, the three-phase dielectric-magnetic-polymer composites offer more choices for devices design. It could facilitate reducing the size of the devices, especially the passive components integrating both capacitors and inductors, such as LC filter, microwave antenna [23] and so on. Several works [22,24,25] have been carried out to develop various magnetic-dielectric-polymer composites with widely adjustable properties. However, the respective effect of different fillers on the dielectric and magnetic performance of the composites, the interfacial status under applied electric field, and the percolation behavior, are still ambiguous. The microwave-absorption properties caused by the magnetic loss and dielectric loss in the three-phase systems have also rarely been reported. A systematic investigation on the above mechanism is crucial for the structure design and miniaturization of the devices.

The purpose of this study is to investigate the magnetic, dielectric and microwave absorption characteristics of the magnetic-polymer and magnetic-dielectric-polymer composites. Sendust (FeAlSi) and $BaTiO_3$ particles are employed as the magnetic and dielectric fillers, respectively. Epoxy resin is used as the polymer matrix because it has excellent mechanical and electrical characteristics, as well as higher load bearing capability compared to some thermoplastics. The influence of volume fractions of FeAlSi and $BaTiO_3$ on the complex permeability and permittivity of the composites were measured and analyzed up to 1 GHz. The dielectric percolation behavior was realized by the field effect on the interface of FeAlSi fillers with COMSOL Multiphysics simulation. The microwave absorption characteristics of the composites are investigated.

2. Experimental

The epoxy (E51: $C_{21}H_{24}O_4$, Jitian Chemical company, China) was employed as the matrix. Micro-sized FeAlSi powers (Commercial, China) and nano-sized $BaTiO_3$ (Commercial, China) were used as functional fillers. In the first step, a certain amount of epoxy was dissolved in Butanone (MEK) solvent. Then a certain amount of FeAlSi and $BaTiO_3$ were added. The solution was slowly stirred and ultrasonicated for thirty minutes. A curing agent (tetraethylene pentamine, China) was added to the above solution and stirred continuously. The fillers were dispersed homogeneously in the solution. The solvent was slowly evaporated until a highly viscous mixture containing fillers, epoxy, and curing agent was obtained. Subsequently, the mixture was poured into a mold with 8 mm inner diameter and 19 mm outer diameter. The sample thickness was about 1 mm. At last, the magnetic slurry was cured at 60 °C for 72 h.

The crystal structure of FeAlSi and $BaTiO_3$ was analyzed using X-ray diffraction (X'Pert PRO MPD, Philips) with Cu K_α radiation, at a scanning speed of 2°/min in steps of 0.02°. The microstructure of the fillers was examined using Scanning electron microscope (SEM) (4800S, Hitachi) and optical microscope (Olympus BX51RF). The magnetic properties of the FeAlSi powder were characterized by a vibrant sample magnetometer (VSM, HH-20, Nanjing NanDa Instrument Plant, 298 K) with a maximum magnetic field of 1.5 T. Complex permeability and permittivity spectra of the composite were measured with impedance analyzer (Agilent 4991) in a frequency range from 10^6 to 10^9 Hz.

3. Results and discussion

3.1. Characterization of FeAlSi and $BaTiO_3$ powders

Fig. 1 shows the X-ray diffraction patterns of the FeAlSi and $BaTiO_3$ powders. Two structures are present in the FeAlSi, as shown in Fig. 1(a): bcc disordered structure α-Fe and DO_3 superlattice ordered structure. It is well known that the DO_3 superlattice structure exhibits excellent soft magnetic properties [26]. The magnetic properties of the FeAlSi alloy depend on the proportion of the two structures. Fig. 1(b) presents that the diffraction peak from {1 0 0} plane of $BaTiO_3$ is not symmetric, which may indicate that both cubic and tetragonal phases coexist in the 100 nm nano particles. The inset shows that the (2 0 0) peak of cubic phase overlapped with (0 0 2) peak of tetragonal ferroelectric phase.

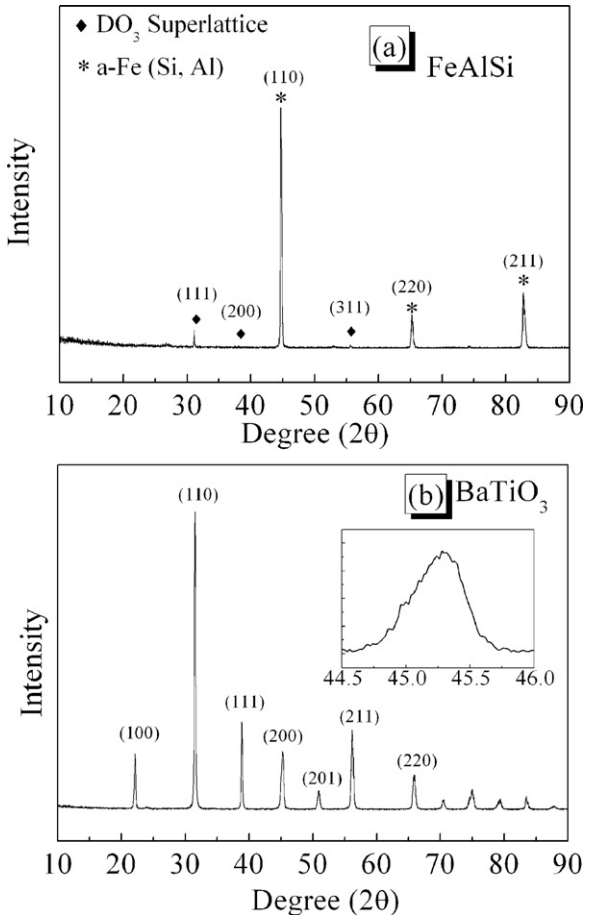

Fig. 1. X-ray diffraction patterns of (a) FeAlSi and (b) $BaTiO_3$ powders, the inset is the (2 0 0) peak of $BaTiO_3$ powder.

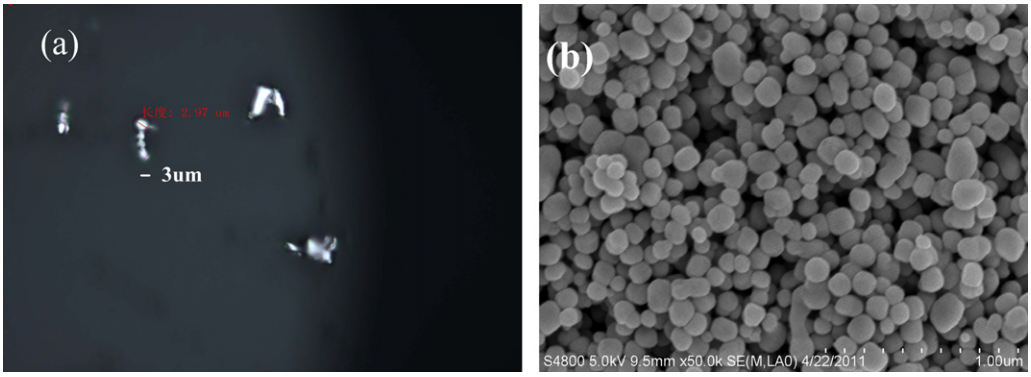

Fig. 2. Microstructure of (a) FeAlSi and (b) $BaTiO_3$ powers.

3.2. Microstructure of FeAlSi powers

Fig. 2 shows the microstructure of the FeAlSi and $BaTiO_3$ powers. As shown in Fig. 2(a), the diameter of the sendust particles is a few of micro-meters, while the size of $BaTiO_3$ is nano-sized, as shown in Fig. 2(b). The shape of the senduct particles is irregular and composed of the clusters with several microns. The shape of $BaTiO_3$ particles is nearly spherical with the size distribution of 100–200 nm.

3.3. Magnetic properties of FeAlSi powders

Fig. 3 illustrates the variation of the magnetization (M) of the powder as a function of applied field (H) at room temperature. It is noted that the saturation magnetization M_s is very close to a value of 140 emu/g, which is much larger than that of the $NiZnFe_2O_4$ (about 80 emu/g) [27] and Fe_3O_4 (about 60 emu/g) [17] magnetic powders.

It is well known that the initial permeability of the magnetic material is related to the saturation magnetization and coercivity by [28]:

$$\mu_i \propto \frac{M_s}{H_s} \tag{1}$$

The high M_s and small H_c lead to high value of permeability and low cutoff frequency for relaxation. The calculated initial permeability is 1318 by the hysteresis loops. The hysteresis loop with a coercivity (H_c) of 8 Oe in Fig. 3 suggests a typical soft magnetic material, which complies with the ferri-magnetic behavior [29].

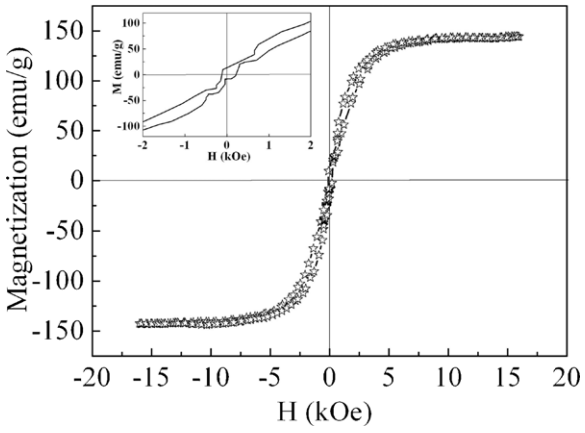

Fig. 3. Magnetic hysteresis loops of the FeAlSi powders.

3.4. Magnetic properties of FeAlSi/epoxy composites

The complex permeability μ^* is an important parameter for the magnetic materials, which can be described as:

$$\mu* = \mu' - j\mu'', \quad j = \sqrt{-1} \tag{2}$$

where $\mu'$and μ'' are the real and imaginary part of permeability, respectively [30].

Fig. 4 shows the frequency dependence of μ' and magnetic loss tan δ_M of the FeAlSi/epoxy composites containing various volumetric fractions of the sendust filler at room temperature. It can be seen that the μ' increases with the sendust filler loading, as shown in Fig. 4(a). The value of μ' increases from 1.18 to 4.0 (10^8 Hz) with the magnetic filler loading increasing from 5 vol% to 50 vol%. The μ' of the composites is nearly frequency-independent with a value of 1.27 and 1.4 while the sendust filler loading is 5 vol% and 6 vol%, respectively. It is slightly decreases with the frequency and this tendency becomes more obvious when the filler loading is higher than 30 vol%. It is worth noting that the plots of permeability versus frequency overlap when the sendust loading is in the range of 45–50 vol%.

The values of tan δ_M for all composites increase with frequency, as shown in Fig. 4 (b). The same phenomena have been reported in other literatures, and this frequency-dependence is related with the dispersion [31], the natural magnetic resonance and eddy current flowing on the surface of the sendust particles [32]. The value of μ' decreases dramatically near the resonance frequency, while tan δ_M rapidly increases because of the increasing of eddy current between the surface of sendust filler and epoxy matrix. As shown in Fig. 4(a) and (b), the plots of μ' and tan δ_M versus frequency with high sendust loading are apparently different from those with low sendust filler loading. The phenomenon may indicate that the composite with high sendust content (45–50 vol%) shows more nature magnetic resonance of FeAlSi fillers.

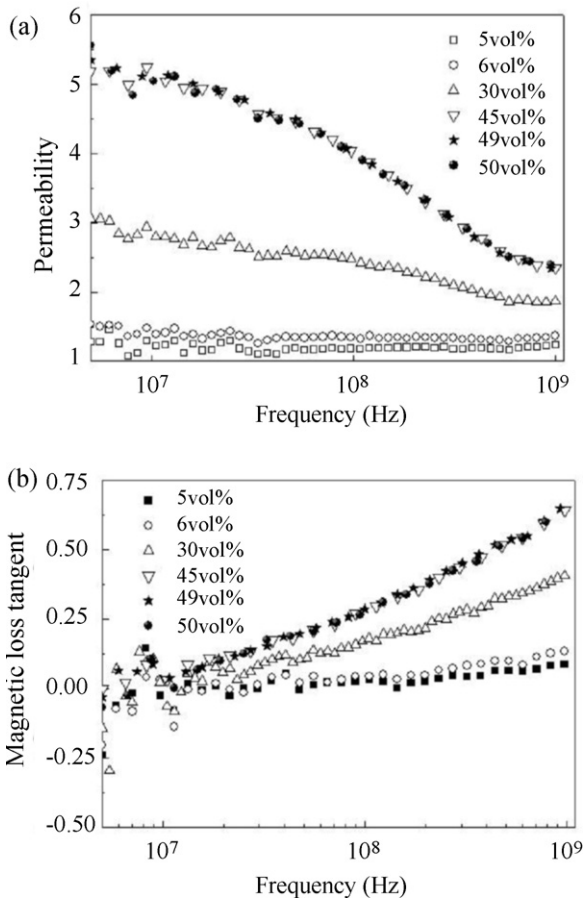

Fig. 4. (a) Real permeability (μ') and (b) magnetic loss tangent (tan δ_M) of FeAlSi/epoxy composites with various FeAlSi volume fractions (f_{FeAlSi}) at room temperature.

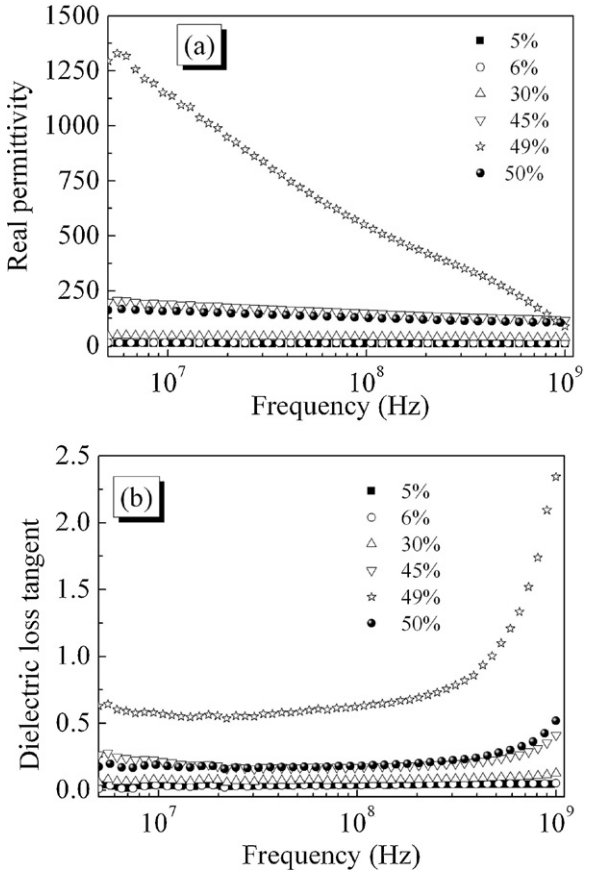

Fig. 5. (a) Real permittivity (ε') and (b) dielectric loss tangent (tan δ_D) of FeAlSi/epoxy composites with various FeAlSi volume fractions (f_{FeAlSi}) at room temperature.

For the sphere-shaped magnetic filler, the Kittel equation has been widely used to calculate the nature resonance frequency of magnetic materials, which is defined as [33]

$$f_r = \gamma H_a \tag{3}$$

where $\gamma = 28$ GHz/T is the gyromagnetic ratio and the anisotropy field is obtained by $H_a = 4|K|/3\mu_0 M_s$, where μ_0 is the vacuum permeability. The saturation magnetization $\mu_0 M_s$ is 0.439 T and the anisotropic coefficient K for the cubic magnetic material is about -9×10^3 J m^{-3} [34]. So the theoretical calculation of the nature resonance frequency for FeAlSi particles should be $\gamma H_a = 0.962$ GHz. This result is in good agreement with the experimental data (~1 GHz) of the composite with 45–50 vol% sendust filler loading. It suggests that the high magnetic loss of the composite should be mainly caused by nature resonance.

Fig. 5 shows the frequency dependence of the permittivity (ε') and dielectric loss tangent (tan δ_D) of the FeAlSi/Epoxy composite with various filler loading at room temperature. A significant increase of ε' from 149 to 547 is observed with f_{FeAlSi} increased from 45 vol% to 49 vol% at 10^8 Hz, as shown in Fig. 5(a). Correspondingly, the tan δ_D increases from 0.17 to 0.62 in Fig. 5(b). As f_{FeAlSi} is further increased to 50 vol%, the ε' and tan δ_D dramatically decrease to 127 and 0.18, respectively. This ultrahigh permittivity with 49 vol% sendust loading indicates the occurrence of percolation behavior. However, similar behavior is not found in the magnetic property, as shown in Fig. 4.

3.5. Magnetic and dielectric properties of FeAlSi/BaTiO$_3$/epoxy composites

Fig. 6 presents the plots of (a) μ' and (b) tan δ_M versus frequency with 6 vol% FeAlSi volume fraction and various $BaTiO_3$ loadings at room temperature. It can be seen that μ' and tan δ_M are nearly independent with the $BaTiO_3$ content because of the fixed volume sendust filler loading. This result shows that the magnetic performance is not affected by the non-magnetic $BaTiO_3$ particles in the three-phase composite. However, the ε' of the FeAlSi/$BaTiO_3$/epoxy composites is enhanced with increasing the $BaTiO_3$ loading.

Fig. 7 shows the frequency dependence of the ε' and tan δ_D of the composites with 6 vol% FeAlSi filler and various $BaTiO_3$ loadings at room temperature. An obvious increase in permittivity is observed with the increase of $BaTiO_3$ loading. The ε' increases from 13 to 18 with the $BaTiO_3$ loading is increased from 0 vol% to 8 vol% at 10^8 Hz. As for the loss tangent of the composites, there is no apparent change for

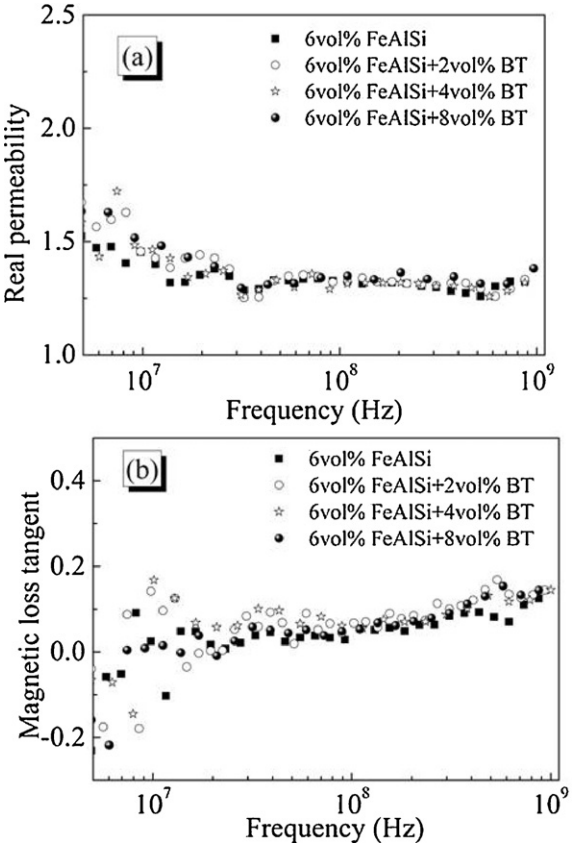

Fig. 6. (a) Real permeability (μ') and (b) magnetic loss tangent ($\tan\delta_M$) of FeAlSi/$BaTiO_3$/epoxy composites with 6 vol% FeAlSi volume fractions and various $BaTiO_3$ (BT) loading at room temperature.

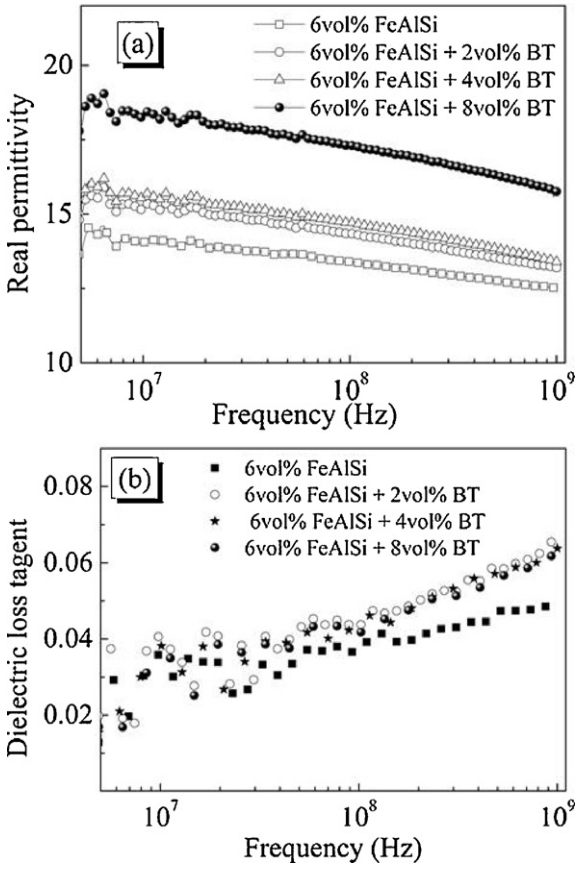

Fig. 7. (a) Real permittivity (ε') and (b) dielectric loss tangent ($\tan\delta_D$) of FeAlSi/epoxy composites with various FeAlSi volume fractions (f_{FeAlSi}) at room temperature.

different composites and it keeps the low value of no more than 0.06 below the frequency of 100 MHz. It suggests good insulation between the conductive sendust fillers, $BaTiO_3$ ceramic particles and epoxy matrix.

The increment of permittivity is mainly contributed by the high permittivity of $BaTiO_3$. The micro-sized magnetic sendust particles are surrounded by the nano-sized $BaTiO_3$ in the composite system. The micro-capacitors composed by the adjacent conductive sendust particles and the $BaTiO_3$ particles in between contribute to a larger capacitance comparing with the FeAlSi/epoxy composite system. The permeability of both $BaTiO_3$ and the polymer matrix is about 1, so the permeability of FeAlSi/$BaTiO_3$/epoxy composite is not dependent on the f_{BaTiO_3} with the same magnetic filler loading.

3.6. Theoretical models of FeAlSi-epoxy composites

The percolation behavior was presented in the dielectric property of the FeAlSi-epoxy composite, however, similar behavior was not found in magnetic performance. In order to clarify the mechanism of the electrical and magnetic properties of the composites, the percolation theory [11] and effective medium theory model (EMT) [35] are used to predict ε_r of the composite at 10^8 Hz and room temperature, with the corresponding Eqs. (4) and (5), respectively. The results are shown in Fig. 8.

$$\varepsilon_r = \varepsilon_1 \left| \frac{(f_c - f)}{f_c} \right|^{-q} \tag{4}$$

$$\mu_r = \mu_1 \left[1 + \frac{f(u_2 - u_1)}{\mu_1 + n(1-f)(\mu_2 - \mu_1)} \right] \tag{5}$$

where ε_r is the real permittivity of the FeAlSi/epoxy composite; ε_1 is the permittivity of the epoxy; u_1 and u_2 are the initial permeability of epoxy and FeAlSi, respectively. The f, f_c, n and q are the volume fraction of the FeAlSi particles, percolative threshold, sendust morphology fitting factor, and critical exponent of about 1, respectively. ε_r and μ_r were measured at 10^8 Hz and room temperature. It is worth noting that the same formulation is also applicable for the permittivity by replacing permeability μ with permittivity ε_r [4].

As shown in Fig. 8(a), the permittivity of the FeAlSi/Epoxy composites increases dramatically with the FeAlSi filler loading from 45 vol% to 49 vol%. This behavior indicates the occurrence of percolation behavior. The experimental results are in good agreement with those calculated by using Eq. (4), where $\varepsilon_1 = 3$ and the derived f_c and q are 49 vol% and 0.93, respectively. This behavior is similar with other conductor-polymer composites [36]. The critical exponent q is considered universally, depending only on the spatial

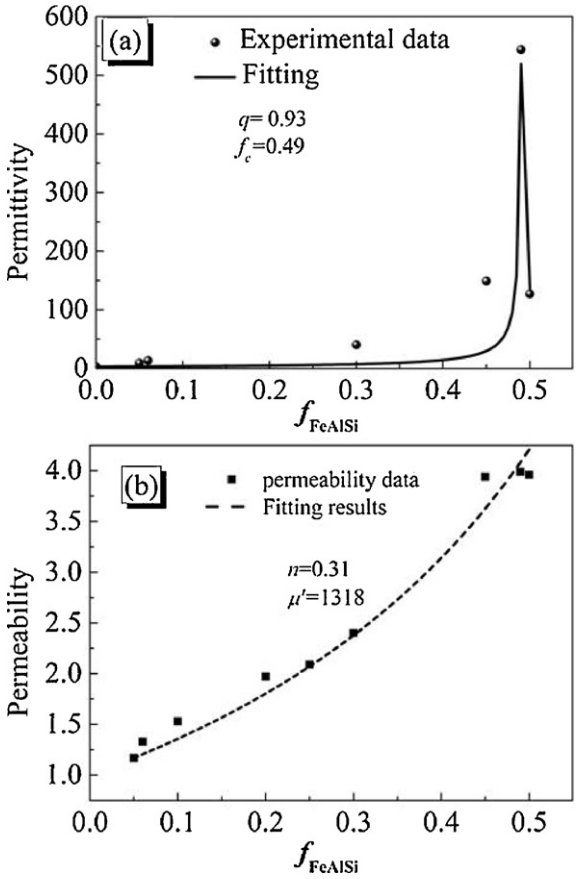

Fig. 8. Experimental and fitted values of (a) ε_r and (b) μ_r of FeAlSi/epoxy composites with different volume fractions of sendust at 10^8 Hz and room temperature.

dimension of the composites. However, reports have shown that the interaction between the conductive fillers in percolative composites also plays an important role in determining the value of q [11]. The $q = 0.93$ derived in this study is slightly deviated from the classic value of ''1'', which shows the slight interaction between magnetic fillers.

As for the permeability of the FeAlSi/epoxy composite, the experimental data are in good agreement with the calculated results by using Eq. (5), where $\mu_1 = 1$, $\mu_2 = 1318$ and the derived n is 0.31. It is worth noting that the value of the morphology fitting factor n (0.31) obtained from the fitting is much higher than that reported previously where the derived n is 0.13 or 0.11 [35], which indicates that the permeability of the FeAlSi/epoxy composite in this study is more associated with the filler size and shape. The deviation of $n = 0.31$ indicating the micro-size of the ceramic filler matches well with the microstructure of the sendust shown in Fig. 2(a). According to the magnetic circuit model, static permeability μ_s is given by [37]:

$$\mu_s = \frac{\mu_i(1 + (\delta/D))}{1 + \mu_i(\delta/D)} \tag{6}$$

where μ_s is the intrinsic static permeability of materials without any defects, δ and D are the thickness of the grain boundaries and average grain size, respectively. In general, the ratio of δ/D decreases with increasing grain size (D), and thus promoting static permeability. For the FeAlSi/epoxy composite, the non-magnetic polymer matrix can be regards as the grain boundary of the sendust, the sendust fillers are surrounded by the polymer matrix. So, increasing the f_{FeAlSi} or the grain size of sendust will lead to the higher permeability of the composite system.

It is noted that the nonlinear mutation presented on permittivity of the FeAlSi/epoxy composite near the percolative threshold is not found in Fig. 8(b). Although the initial permeability μ_i of FeAlSi is 1318, the permeability of the composite with $f_{FeAlSi} = 50$ vol% still keeps a low level of $\mu' = 4.0$. Similar results were obtained in other magnetic-polymer composites [38]. These results suggest that the insulation polymer matrix drastically deteriorates the continuity of the magnetizing. This pronounced reduction in permeability is still puzzling and has been intensively discussed in the literature [39]. Studies have shown that 5% non-magnetic matrix reduces the permeability of soft magnetic composite by more than 75% [40]. On the other hand, if the matrix is magnetic and the fillers are non-magnetic, the μ' of the composites will decrease nearly linearly with increasing the non-magnetic volume fraction. Actually, the permeability of the composite more strongly depends on the matrix than on the fillers. Besides that, even at low porosity levels, the μ' of the composite will decrease dramatically.

3.7. Effect of electric field on the surface of FeAlSi and $BaTiO_3$ fillers in the two and three-phase composites

In order to examine the field effect on the interface of the FeAlSi/epoxy, a 2D modeling is used to represent FeAlSi filler with $f_{FeAlSi} = 49$ vol% (percolation threshold) in epoxy matrix, which is shown in Fig. 9. The model is based on the dielectric theory [41]:

$$\boldsymbol{E} = \frac{\boldsymbol{U}}{\boldsymbol{d}} \tag{7}$$

$$\boldsymbol{D} = \varepsilon_0 \boldsymbol{E} + \boldsymbol{P} \tag{8}$$

$$\boldsymbol{P} = \varepsilon_0(\varepsilon_{effect} - 1)\boldsymbol{E} \tag{9}$$

$$\boldsymbol{W_e} = \frac{1}{2}\boldsymbol{DE} \tag{10}$$

where $\boldsymbol{U}$ is applied voltage, $\boldsymbol{E}$ and $\boldsymbol{d}$ are electric field and distance between plates, respectively. $\boldsymbol{D}$, $\boldsymbol{P}$, $\boldsymbol{W_e}$, ε_0 and ε_{effect} are electric displacement, dielectric polarization and electric energy density, permittivity of free space and effective permittivity respectively. The input voltage (5 V), permittivity of epoxy $\varepsilon_1 = 3$ and sendust $\varepsilon_{FeAlSi} = 10^6$ were used as the parameter to simulate the electric properties of the composite. It is found that the free electrons in the composite, especially the bound electrons of FeAlSi filler, were gathered at the surface of FeAlSi fillers in the presence of 5 V applied, which results in a higher electric field ($\boldsymbol{E}$) at the surface of FeAlSi filler in the direction of voltage as shown in Fig. 9(a). Correspondingly, the higher electric energy density (Fig. 9(b)) and polarization (Fig. 9(c)) are deduced from the higher $\boldsymbol{E}$ at the surface of FeAlSi filler, which means high permittivity and loss FeAlSi/epoxy composite

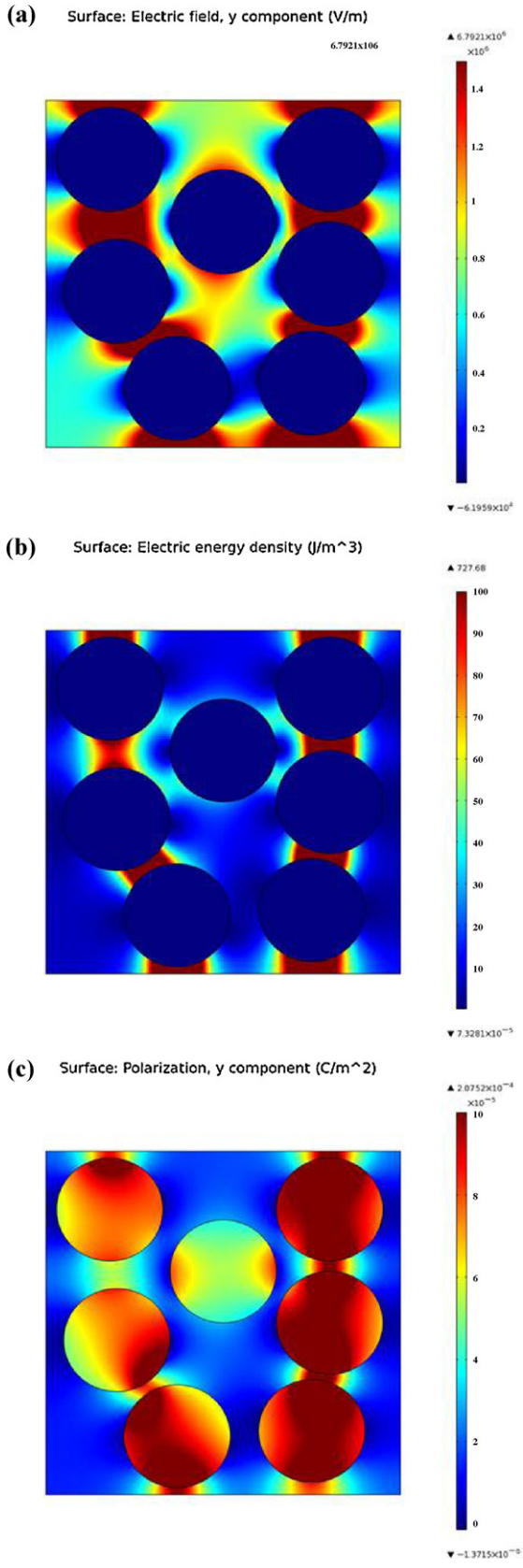

Fig. 9. (a) Electric field, (b) electric energy density and (c) polarization in the FeAlSi-epoxy composite with f_{FeAlSi} = 49 vol%.

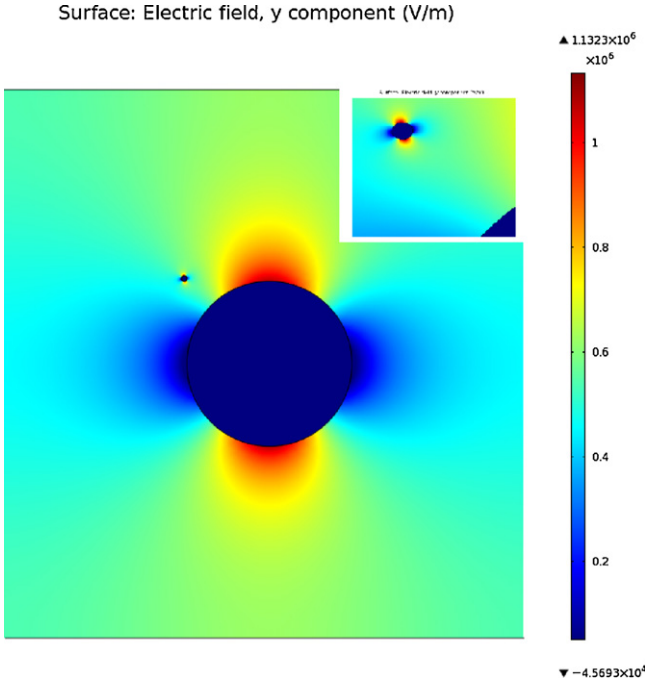

Fig. 10. An illustration of electric field effect at the surface of FeAlSi and $BaTiO_3$ fillers in FeAlSi/$BaTiO_3$/epoxy composite (The inset is the electric field effect at the surface of $BaTiO_3$). The little circle represents the $BaTiO_3$ filler and the large one is FeAlSi.

at the percolation threshold. Combining with the theoretical analysis, the derived q according to the percolation theory deviates from the classic value "1" indicating the slight interaction between the sendust particles in the composite.

As for the FeAlSi/$BaTiO_3$/epoxy composite, as shown in Fig. 10, the maximum of the electric field on the surface of $BaTiO_3$ (Fig. 10, in inset) deviate from the direction of the electric field applied on the composite, whereas the field on the FeAlSi filler is not affected, indicating weak coupling effect between the FeAlSi and $BaTiO_3$ fillers.

3.8. Microwave absorption properties of FeAlSi/$BaTiO_3$/epoxy composites

In order to study the microwave absorption properties, simulations were conducted on the FeAlSi/epoxy and FeAlSi/$BaTiO_3$/Epoxy composites. The simulations were performed in a wide frequency range from 0.05 to 27 GHz. The complex values of ε and μ for simulation in the frequency range of 1–27 GHz employed the experimental data obtained at 1 GHz. The relation between the reflection of the composite and the microwave frequency can be expressed by [33]:

$$z_{in} = \sqrt{\frac{u_r}{\varepsilon_r}}\tanh\left[i\frac{2\pi\omega d\sqrt{u_r\varepsilon_r}}{c}\right] \quad (11)$$

$$R_L(dB) = 20\lg\left|\frac{Z_{in}-1}{Z_{in}+1}\right| \quad (12)$$

where Z_{in} is the normalized input impedance at the absorber surface, μ_r is the relative complex permeability, ε_r is the complex permittivity of the composite, c, ω and d are the

speed of light, frequency of microwaves and the thickness of the absorber, respectively. R_L is reflection loss.

Fig. 11(a) shows the calculated results of reflection loss versus frequency for the FeAlSi/epoxy composites with a layer thickness of 4 mm. It can be seen that the position of the absorbing peak (at 6 GHz with 5 vol%) shifts to low frequency (at 1 GHz with 50 vol%) along with the increasing sendust fraction volume. The changes of the permeability and permittivity are the primary reason for this phenomenon. The reflection loss is almost keeping a constant in the range of 2.5–27 GHz near the percolation threshold (f_{FeAlSi} = 49 vol%), which is apparently different from the composites with low volume fraction. The reason for this behavior is that the giant permittivity near the percolation threshold makes the impedance between the air and the composite deviate from the initial impedance matching condition [42]. In the low volume fraction, the high conductive sendust particles were separated by the non-magnetic polymer matrix, which results in the reduction of permeability and permittivity for the composite compared with the bulk sendust material. However, as for the composite near the percolation threshold, the permittivity is dramatically increased, which leads to the value of $\tanh[(2i\pi fd\sqrt{u_r\varepsilon_r})/c]$ close to "1" in the wide frequency range from 2.5 to 27 GHz. In addition to the complex permittivity and permeability, the thickness (d) of the sample also affects the reflection loss of the composite [43], as shown in Fig. 11(b). With increasing sample thickness, the position of first absorption peaks shifts to lower frequency, while the value of absorption peaks increases with the thickness increased from 1 to 5 mm.

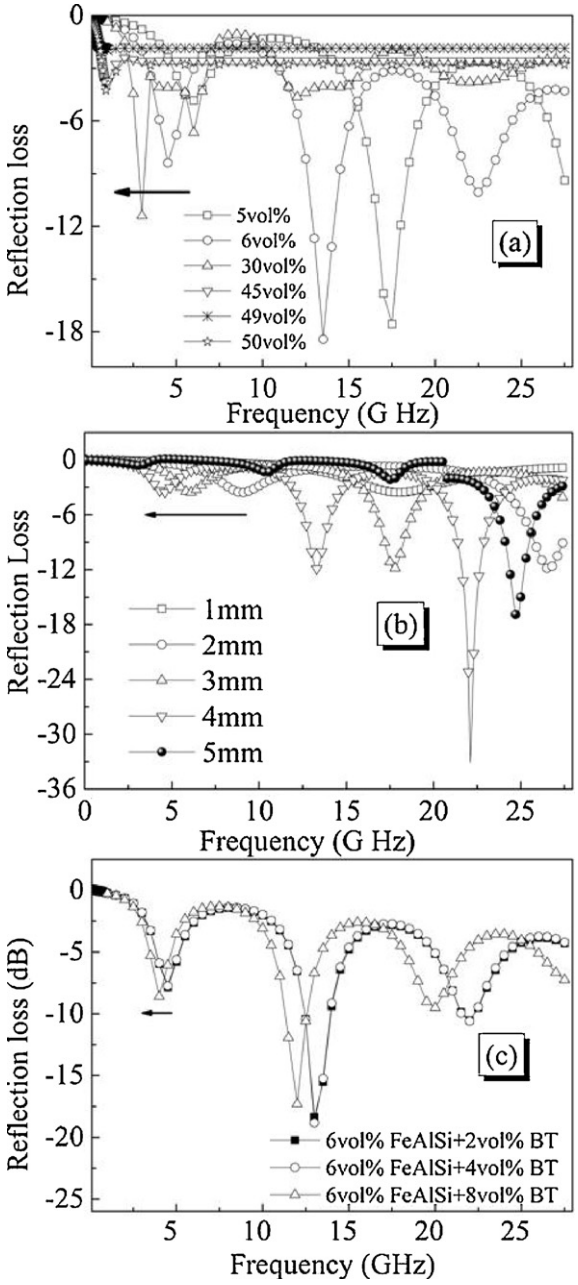

Fig. 11. Reflection loss of FeAlSi/epoxy composite (a) with various volume fractions for a layer thickness of 4 mm and (b) 6 vol% FeAlSi with various layer thicknesses. (c) FeAlSi-$BaTiO_3$-epoxy composite with 6 vol% FeAlSi and various volume fractions of $BaTiO_3$.

In contrast, the Fig. 11(c) shows the impact of permittivity on the reflection loss for FeAlSi-$BaTiO_3$-epoxy composite. It can be seen that the first absorbing peak position shifts from 4.5 GHz to 4 GHz with the $BaTiO_3$ loading increasing from 2 vol% to 8 vol%. And, the peak value of reflection loss decreases from −7.5 dB to −9 dB, which is ascribed to the increased permittivity.

By the laws of physics, this magneto-dielectric polymer composite may have potential applications for miniaturization of antennas and embedded devices (such as filter, splitter and so on). The refractive index $n = \sqrt{u_r \times \varepsilon_r}$ relates to the miniaturization. As for the antenna miniaturization, the high permittivity materials with high permeability are expected. Much research has concentrated on achieving high permittivity, which however, results in low efficiency and narrowband. Besides, if the impedance $((Z/Z_0) = \sqrt{(u_r/\varepsilon_r)})$ is very low, it will be difficult in impedance matching for the antennas with free space. This behavior becomes obvious near the percolation threshold for the FeAlSi/epoxy composite system with extremely high permittivity. For the application of antennas, the ratio of f_{FeAlSi} and f_{BT} should be adjusted to get the characteristic impedance value about 1. As for the embedded device applications, for example low pass filter, the high permittivity and permeability are significant to reduce the size of the devices.

4. Conclusion

The FeAlSi/epoxy and FeAlSi/$BaTiO_3$/epoxy composites with various volume fractions of FeAlSi and $BaTiO_3$ fillers have been successfully prepared. The complex permittivity, permeability and their relationship with microwave absorption properties were investigated. It is found that the ε' of the FeAlSi/epoxy composite increases from 149 to 547 with f_{FeAlSi} increasing from 45 vol% to 49 vol% at 10^8 Hz. However, this percolation effect is not observed in the magnetic behavior of the FeAlSi/epoxy composites. The μ' increases from 1.18 to 4.0 (10^8 Hz) with the f_{FeAlSi} increasing from 5 vol% to 50 vol%. The 2D modeling shows that the high electric energy density is

responsible for this high permittivity near the percolation threshold. In contrast, the μ' of FeAlSi/$BaTiO_3$/epoxy composites with f_{FeAlSi} = 6 vol% is independent on the f_{BT}. However, the ε' increases from 13 to 18 with the f_{BT} increased from 0 vol% to 8 vol%. Theoretical calculations show that the increment of the FeAlSi and $BaTiO_3$ loading, as well as the thickness will cause the absorption peak position moves to lower frequencies. Furthermore, the results suggest a new type of microwave absorptive material with adjustable peak absorption frequency, and its potential applications in embedded devices with reduced physical dimensions.

Acknowledgements

The present research is supported by the National Natural Science Foundation of China (Nos. 50807038 and 20971089) and the research funding from National S&T Major Project with the contract no. 2009ZX02038 and 2009ZX02026.

References

[1] K.J. Lee, M. Damani, R.V. Pucha, S.K. Bhattacharya, R.R. Tummala, S.K. Sitaraman, Reliability modeling and assessment of embedded capacitors in organic substrates. Components and packaging technologies, IEEE Trans. Comp. Pack. Technol. 30 (1) (2007) 152–162.

[2] X. Zhang, W. Ren, P. Shi, M.S. Khan, X. Chen, X. Wu, X. Yao, Preparation and electrical properties of $Bi_2Zn_{2/3}Nb_{4/3}O_7$ thin films deposited at room temperature for embedded capacitor applications, Ceram. Int. (2011), doi:10.1016/j.ceramint.2011.04.053.

[3] L. Ramajo, M.M. Reboredo, M.S. Castro, $BaTiO_3$ – epoxy composites for electronic applications, Int. J. Appl. Ceram. Technol. 7 (2010) 444–451.

[4] H.C. Pant, M.K. Patra, A. Verma, S.R. Vadera, N. Kumar, Study of the dielectric properties of barium titanate polymer composites, Acta Mater. 54 (2006) 3163–3169.

[5] W. Yang, S. Yu, R. Sun, R. Du, Nano- and microsize effect of CCTO fillers on the dielectric behavior of CCTO/PVDF composites, Acta Mater. 59 (2011) 5593–5602.

[6] G.M. Odegard, Constitutive modeling of piezoelectric polymer composites, Acta Mater. 52 (2004) 5315–5330.

[7] P. Xu, X. Han, C. Wang, D. Zhou, Z. Lv, A. Wen, X. Wang, B. Zhang, Synthesis of electromagnetic functionalized nickel/polypyrrole core/shell composites, J. Phys. Chem. B 112 (2008) 10443–10448.

[8] T.I.Y.A. Kofinas, Controlled synthesis of core–shell iron–silica nanoparticles and their magneto-dielectric properties in polymer composites, Nanotechnology 22 (2011) 105601.

[9] Y. Hou, Y. Cheng, T. Hobson, J. Liu, Design and synthesis of hierarchical MnO_2 nanospheres/carbon nanotubes/conducting polymer ternary composite for high performance electrochemical electrodes, Nano Lett. 10 (2010) 2727–2733.

[10] S. Mitra, O. Mondal, D.R. Saha, A. Datta, S. Banerjee, D. Chakravorty, magnetodielectric effect in Graphene-PVA nanocomposites, J. Phys. Chem. C 115 (2011) 14285–14289.

[11] C.W. Nan, Y. Shen, J. Ma, Physical properties of composites near percolation, Annu. Rev. Mater. Res. 40 (2010) 131–151.

[12] C.G. Robertson, C.J. Lin, M. Rackaitis, C.M. Roland, Influence of particle size and polymer–filler coupling on viscoelastic glass transition of particle-reinforced polymers, Macromolecules 41 (2008) 2727–2731.

[13] W. Zhou, D. Yu, Thermal and dielectric properties of the aluminum particle/epoxy resin composites, J. Appl. Polym. Sci. 118 (2010) 3156–3166.

[14] Z. Ghallabi, H. Rekik, S. Boufi, M. Arous, A. Kallel, Effect of the interface treatment on the dielectric behavior of composite materials of unsaturated polyester reinforced by Alfa fiber, J. Non-Cryst. Solids 356 (2010) 684–687.

[15] K. Lee, Y. Yun, S. Kim, S. Kim, Microwave absorption of λ/4 wave absorbers using high permeability magnetic composites in quasimicrowave frequency band, J. Appl. Phys. 103 (2008), 07E504-3.

[16] R. MouCka, J. VilCakova, N.E. Kazantseva, A.V. Lopatin, P. Saha, The influence of interfaces on the dielectric properties of MnZn-based hybrid polymer composites, J. Appl. Phys. 104 (2008) 103718–103811.

[17] L.A. Ramajo, A.A. Cristóbal, P.M. Botta, J.M. Porto López, M.M. Reboredo, M.S. Castro, Dielectric and magnetic response of Fe_3O_4/epoxy composites, Composites A 40 (2009) 388–393.

[18] R. Dosoudil, M. Usakova, J. Franek, J. Slama, A. Gruskova, Particle, Size and concentration effect on permeability and EM-Wave absorption properties of hybrid ferrite polymer composites, IEEE Trans. Magn. 46 (2010) 436–439.

[19] B. Li, Y. Shen, Z. Yue, C. Nan, High-frequency magnetic and dielectric properties of a three-phase composite of nickel, Co_2Z ferrite and polymer, J. Appl. Phys. 99 (2006) 123909–123916.

[20] Y. Shirakata, N. Hidaka, M. Ishitsuka, A. Teramoto, T. Ohmi, Low-loss composite material containing fine Zn-Ni-Fe flakes for high-frequency applications, IEEE Trans. Magn. 45 (2009) 4337–4340.

[21] T.J. Fiske, H. Gokturk, D.M. Kalyon, Enhancement of the relative magnetic permeability of polymeric composites with hybrid particulate fillers, J. Appl. Polym. Sci. 65 (1997) 1371–1377.

[22] Z. Guo, S.E. Lee, H. Kim, S. Park, H.T. Hahn, A.B. Karki, D.P. Young, Fabrication, characterization and microwave properties of polyurethane nanocomposites reinforced with iron oxide and barium titanate nanoparticles, Acta Mater. 57 (2009) 267–277.

[23] J. Juuti, M. Teirikangas, K. Sonoda, H. Jantunen, Thermoplastic 0-3 ceramic polymer composites with adjustable magnetic and dielectric characteristics for radio frequency applications, J. Appl. Ceram. Technol. 7 (2010) 452–460.

[24] F. Rasoanoavy, V. Laur, S. De Blasi, J. Lezaca, P. Queffelec, K. Garello, B. Viala, Magnetodielectric effect in trilayered $Co_{65}Fe_{35}B_{20}$/PVDF/$Co_{65}Fe_{35}B_{20}$ composite materials prediction and measurement for tunable microwave applications, J. Appl. Phys. 107 (2010), 09E313-3.

[25] H. Yang, H. Wang, F. Xiang, X. Yao, Multifunctional $SrTiO_3$/NiZn ferrite/POE composites with eletromagnetic and flexible properties for RF applications, J. Electroceram. 22 (2009) 221–226.

[26] M. Miyazaki, M. Ichikawa, T. Komatsu, K. Matusita, Mossbauer effect study of ordering in Fe-Al-Si and Fe-Al-Si-Ni magnetic thin films, IEEE Trans. Magn. 28 (1992) 2430–2432.

[27] M. Jalaly, M.H. Enayati, F. Karimzadeh, P. Kameli, Mechanosynthesis of nanostructured magnetic Ni–Zn ferrite, Powder Technol. 193 (2009) 150–153.

[28] K. Garello, E. Benevent, J.P. Michel, D. Cros, B. Viala, Magnetodielectric thin film heterostructure with high permeability and permittivity, IEEE Trans. Magn. 45 (2009) 4325–4328.

[29] K. Sakai, N. Asano, Y. Wada, S. Yoshikado, Composite electromagnetic wave absorber made of soft magnetic material and polystyrene resin and control of permeability and permittivity, J. Eur. Ceram. Soc. 30 (2010) 347–353.

[30] A. Thakur, P. Thakur, J. Hsu, Novel magnetodielectric nanomaterials with matching permeability and permittivity for the very-high-frequency applications, Scr. Mater. 64 (2011) 205–208.

[31] T.D. Zhou, P.H. Zhou, D.F. Liang, L.J. Deng, Structure and electromagnetic characteristics of flaky FeSiAl powders made by melt-quenching, J. Alloys Compd. 484 (2009) 545–549.

[32] T. Yamane, A. Nishikata, Y. Shimizu, Resonance suppression of a spherical electromagnetic shielding enclosure by using conductive dielectrics, IEEE Trans. Electromagn. 42 (2000) 441–448.

[33] S. Ni, S. Lin, Q. Pan, F. Yang, K. Huang, D. He, Hydrothermal synthesis and microwave absorption properties of Fe_3O_4 mnanocrystals, J. Phys. D: Appl. Phys. 42 (2009) 055004.

[34] C. Kittel, On the theory of ferromagnetic resonance absorption, Phys. Rev. 73 (1948) 155–161.

[35] R. Yang, Q. Jianmin, T. Marinis, C.P. Wong, A precise numerical prediction of effective dielectric constant for polymer-ceramic composite based on effective-medium theory, IEEE Trans. Comp. Pack. Technol. 23 (2000) 680–683.

[36] W. Yang, S. Yu, R. Sun, S. Ke, H. Huang, R. Du, Electrical modulus analysis on the Ni/CCTO/PVDF system near the percolation threshold, J. Phys. D: Appl. Phys. 44 (2011) 475305.
[37] Q. Feng, J. Yang, S. Fu, Y. Mai, Synthesis of carbon nanotube/epoxy composite films with a high nanotube loading by a mixed-curing-agent assisted layer-by-layer method and their electrical conductivity, Carbon 48 (2010) 2057–2062.
[38] Y. Shen, Z. Yue, M. Li, C.W. Nan, Enhanced initial permeability and dielectric constant in a double-percolating $Ni_{0.3}Zn_{0.7}Fe_{1.95}O_4$ polymer composite, Adv. Funct. Mater. 15 (2005) 1100–1103.
[39] Y. Pittini-Yamada, E.A. Perigo, Y. de Hazan, S. Nakahara, Permeability of hybrid soft magnetic composites, Acta Mater. 59 (2011) 4291–4302.
[40] L.B. Kong, Z.W. Li, G.Q. Lin, Y.B. Gan, Electrical and magnetic properties of magnesium ferrite ceramics doped with Bi_2O_3, Acta Mater. 55 (2007) 6561–6572.
[41] M.T. Johnson, E.G. Visser, A coherent model for the complex permeability in polycrystalline ferrites, IEEE Trans. Magn. 26 (1990) 1987–1989.
[42] M. Cao, W. Song, Z. Hou, B. Wen, J. Yuan, The effects of temperature and frequency on the dielectric properties, electromagnetic interference shielding and microwave-absorption of short carbon fiber/silica composites, Carbon 48 (2010) 788–796.
[43] F. Ma, Y. Qin, F. Wang, D. Xue, The architecture assembled from Ni nanocones and its microwave-absorbing properties, Scr. Mater. 63 (2010) 1145–1148.